

Consolidation and Expansion of a Granular Bed of Superabsorbent Hydrogels

Eiji Iritani, Nobuyuki Katagiri, Kyong-Min Yoo, and Hirotoshi Hayashi

Dept. of Chemical Engineering, Nagoya University, Nagoya 464-8603, Japan

DOI 10.1002/aic.11045

Published online November 15, 2006 in Wiley InterScience (www.interscience.wiley.com).

Both consolidation and expansion properties of a packed bed of superabsorbent hydrogel particles under the action of the mechanical loads were investigated in various ionic environments using a KCl solution to clarify the role of the osmotic pressure of the solution on the deformation behaviors of hydrogel particles. A description of the consolidation process was accomplished through the use of either the modified Terzaghi model or a simplified computation method. As the concentration of KCl solution increased, the consolidation rate increased and the packed hydrogels became denser. The data were well analyzed based on the idea of the effective osmotic pressure of the solution. Moreover, in the expansion process of the compressed bed of hydrogel particles, it was determined that the secondary expansion effect known as the creep effect plays an important role on the expansion behavior. It was found that expansion proceeds more slowly than consolidation. © 2006 American Institute of Chemical Engineers AIChE J, 53: 129–137, 2007

Keywords: consolidation, expansion, hydrogel, osmotic pressure, creep effect

Introduction

Superabsorbent crosslinked hydrogels, which undergo a drastic change in volume by absorbing several hundred times their own weight of water while still remaining insoluble, have been developed, and they are increasingly being used as a water preservation agent for sanitary and agricultural uses. It is well known that the ionic environment of the solution has a significant effect on the dynamic behaviors of hydrogel particles swelling in the solution.¹ For a practical use of hydrogels, it is of particular importance to understand how packed hydrogel particles are deformed under the combination of the mechanical load and the electrolyte solution.

Although there have been a number of studies on consolidation of compressible solid cakes, much of this work has been devoted to analyzing consolidation behaviors on the hard materials such as clay and industrial mineral slurry, with less work focused on consolidation of the soft materials. For example, Shirato et al.² used the modified Terzaghi model to analyze the primary consolidation of clay. More-

over, they developed the Terzaghi–Voigt combined model to evaluate the secondary consolidation.

Consolidation of the soft materials such as gel^{3,4} and biological materials⁵ has become important in recent years. It was reported that the consolidation process of agar-agar gel was analyzed based on the modified Terzaghi model.⁶ Lanoi-sellé et al.⁷ developed the model for describing the mechanical consolidation of cellular materials by considering the liquid transfer within a network of three different volumes: extraparticle, extracellular, and intracellular volumes. Chang and Lee⁸ analyzed a constant-rate consolidation period that appears in the final phase of expression of biological sludge. They speculated that this behavior arises from the release of strongly bound water from the biological particles. Deformation behaviors of a gel have been studied under the imposition of shear.⁹ The water permeability of the gel, which is important in describing the deformation behaviors of the gel, has been evaluated.¹⁰ It was reported that the consolidation and expansion behaviors of packed hydrogels under mechanical loads were examined on the basis of the modified Terzaghi model.¹¹ More recently, Lu et al.¹² examined the deformation behaviors of deformable particles under hydraulic drag and mechanical load using calcium-alginate gel particles.

Correspondence concerning this article should be addressed to E. Iritani at iritani@nuce.nagoya-u.ac.jp.

The key objective of this current work is to examine the combined effects of various mechanical pressures and salt concentrations on the consolidation and expansion properties of packed beds of hydrogel particles. We attempt to develop a method for correlating data obtained from experiments of consolidation and expansion of packed hydrogels by introducing the idea of the effective osmotic pressure of the solution. The creep effect in both processes is evaluated based on either the modified Terzaghi model, the Terzaghi–Voigt model, or the simplified computation method.

Experimental

Materials

The superabsorbent gel examined in this research is a commercially available spherical gel (Aqua Pearl, A-grade, Mitsubishi Chemical Corp., Tokyo, Japan) of crosslinked sodium polyacrylate, which has $-\text{COONa}$ groups fixed on the gel network as a functional group. After powdered gel particles were sieved by using a Rotap sieve shaker, the gels with a mean specific surface area size of $321 \mu\text{m}$ were used in all experiments. The swelled hydrogels were prepared by immersing preweighed quantities of the dry gel particles in ultrapure water or KCl solutions of different concentrations.

Experimental apparatus and technique

The experiments were performed by using the so-called compression–permeability (C-P) cell,¹³ which consisted of a cell cylinder and a piston with a cross-sectional area of 28.3 cm^2 . The liquid can flow out of or into the granular bed of hydrogels through the top and bottom filter media under application of a mechanical load by means of a piston. The swelled hydrogel particles were loaded into and then preconsolidated in the C-P cell under a pressure p_1 of 98 kPa, resulting in a semisolid material with a uniform void ratio, subsequently followed by consolidation at a set pressure p_2 in the range of 196–1962 kPa. After the material reached its equilibrium compressibility limit for the given applied pressure p_2 , the pressure was reduced to a pressure p_1 of 98 kPa instantaneously, allowing the cake to expand and swell under a condition in which the cake was saturated with liquid. Variations of the cake thickness over time during both consolidation and expansion of the cake were measured by a dial gauge fitted onto the cell cylinder.

Results and Discussion

Consolidation behaviors of packed hydrogels

Figure 1 presents the typical data obtained in consolidation of the granular bed of the swelled superabsorbent hydrogels. The homogeneous semisolid material that was preconsolidated at a pressure of 98 kPa was consolidated at a consolidation pressure of 491 kPa under the condition of a salt concentration of 0.1 mol/L. The average consolidation ratio U_c defined by $U_c = (L_1 - L)/(L_1 - L_\infty)$, indicating a measure of the average degree of consolidation over the total thickness, is plotted against the square root of the consolidation time θ_c , where L_1 , L , and L_∞ are, respectively, the thickness of the compressed cake at $\theta_c = 0$, $\theta_c = \theta_c$, and $\theta_c = \infty$. It is

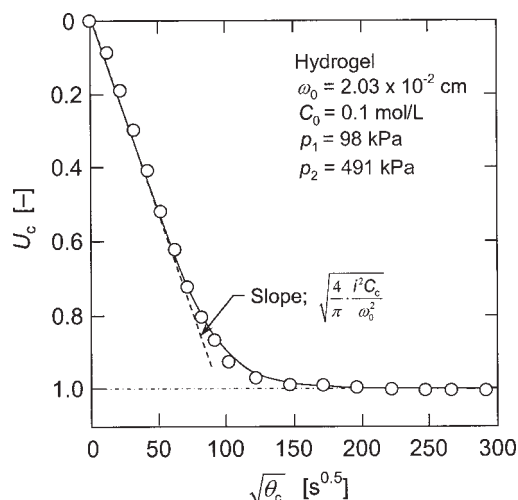


Figure 1. Determination of modified consolidation coefficient C_c .

apparent that U_c is directly proportional to the square root of the consolidation time θ_c in the initial period of consolidation and approaches unity asymptotically as time proceeds. On the basic assumption that the creep effect¹⁴ known as the secondary consolidation effect is negligible, the modified Terzaghi model was applied to analyze the experimental data of the consolidation process. The assumption was also made that the modified consolidation coefficient C_c defined by $C_c = 1/[\mu\rho_s\alpha(-de/dp_s)]$ is constant throughout the cake at any instant, where μ is the viscosity of liquid, ρ_s is the true density of solids, α is the local specific resistance of the material, e is the local void ratio of cake, and p_s is the local solid compressive pressure. Under these assumptions, the average consolidation ratio U_c for constant-pressure consolidation of homogeneous semisolid materials may be given by²

$$U_c = 1 - \sum_{N=1}^{\infty} \frac{8}{(2N-1)^2\pi^2} \exp\left[-\frac{(2N-1)^2\pi^2 i^2 C_c \theta_c}{4\omega_0^2}\right] \quad (1)$$

This is equivalent to

$$U_c = \sqrt{\frac{4 i^2 C_c \theta_c}{\pi \omega_0^2}} + \sqrt{\frac{4 i^2 C_c}{\pi \omega_0^2}} \sum_{N=1}^{\infty} (-1)^N \int_0^{\theta_c} \frac{\exp[-N^2 \omega_0^2 / (i^2 C_c \theta_c)]}{\sqrt{\theta_c}} d\theta_c \quad (2)$$

where i is the number of drainage surfaces and ω_0 is the total solid volume per unit cross-sectional area. For small values of θ_c , Eq. 2 may be approximated by

$$U_c = \sqrt{\frac{4 i^2 C_c \theta_c}{\pi \omega_0^2}} \quad (3)$$

As a consequence, the value of C_c can be determined from the slope of the line in the early stage of the experimental data, as shown in the figure.

Plots of U_c as a function of the square root of $i^2\theta_c/\omega_0^2$ are shown for several different values of the salt concentration C_0 in Figure 2. The figure indicates that the consolidation rate undergoes a significant increase as the salt concentration C_0 increases. However, at concentrations > 0.3 mol/L, the salt concentration unexpectedly ceases to affect the consolidation rate. The solid curves are the calculated values derived based on Eq. 1, using the values of C_c determined by the method shown in Figure 1. Fairly good agreement with all experimental data could be obtained, indicating that the material had no creep characteristics.

To evaluate the consolidation behaviors of homogeneous semisolid materials, the following simplified, semitheoretical equation may also be used instead of Eq. 1¹⁵:

$$U_c = \sqrt{\frac{4i^2C_c\theta_c}{\pi\omega_0^2}} \left/ \left[1 + \left(\frac{4i^2C_c\theta_c}{\pi\omega_0^2} \right)^{\nu/(2\nu)} \right] \right. \quad (4)$$

where ν is the consolidation behavior index that quantifies the creep effect of the material. Sivaram and Swamee¹⁶ presented the above equation with $\nu = 2.8$ on purely empirical grounds. Provided the material has no creep characteristics, the value of ν is 2.85. With a smaller value of ν the creep characteristics become more pronounced.

In Figure 3, the experimental data shown previously in Figure 2 are compared with the calculations based on Eq. 4. The calculations are in good agreement with the experimental data by putting the value of ν as 2.85. Thus, it appears that the creep effect is negligible in consolidation of the packed hydrogels used in this research.

From a practical perspective, the liquid content of packed hydrogels is an important factor in the design and operation of the process relating to hydrogels. Figure 4 compares the experimental data with the calculations of the variations with time of the average void ratio e_{av} , defined as the ratio of void to solid volume of the compressed cake during the consolidation period. It can be seen that the addition of salt has a pronounced effect on the void ratio of the cake. Obviously as the salt concentration increases, packed hydrogels become

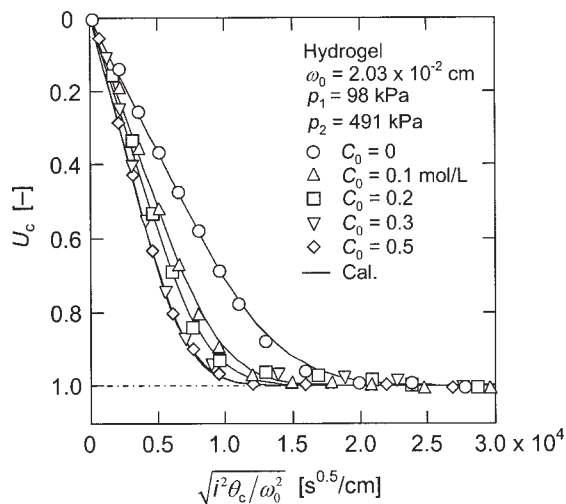


Figure 2. Evaluation of average consolidation ratio U_c based on modified Terzaghi model.

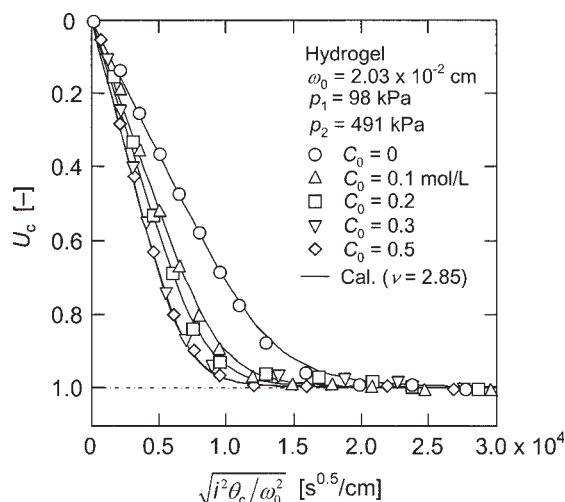


Figure 3. Evaluation of average consolidation ratio U_c based on simplified computation method.

denser and cake behavior undergoes little change during consolidation. Interestingly, qualitatively similar behavior resulting from the salt concentration has been observed by Nakano et al.¹ for swelling of a gel immersed in a salt solution in the absence of the mechanical loads. The solid curves in the figure have been derived from calculated values based on

$$e_{av} = \frac{1}{\omega_0} [L_1 - (L_1 - L_\infty)U_c] - 1 \quad (5)$$

The value of U_c that appears in the above equation was evaluated from Eq. 1.

Figure 5 examines the effects of changing the salt concentration C_0 on the calculated values of the modified consolidation coefficient C_c arising from experimental data using the method shown in Figure 1. The value of C_c tends to increase almost linearly with the increase in C_0 , but concentrations exceeding 0.3 mol/L increase C_c hardly at all.

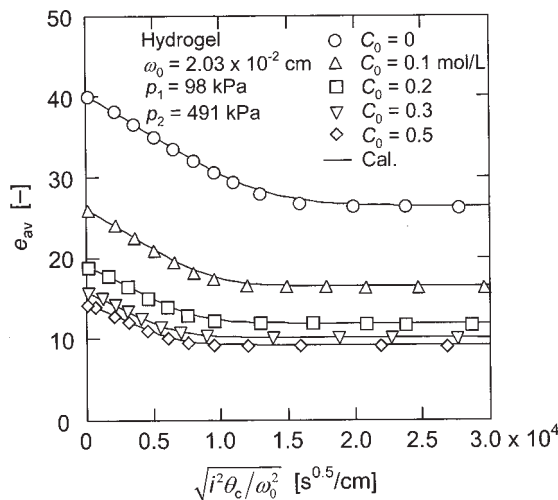


Figure 4. Variations of average void ratio e_{av} of cake with time during consolidation.

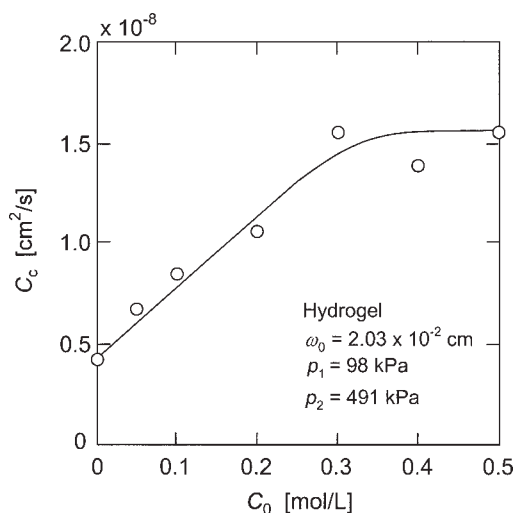


Figure 5. Influence of salt concentration C_0 on modified consolidation coefficient C_c .

Effective osmotic pressure

In general, the modified consolidation coefficient C_c is represented by a unique function of the average solid compressive pressure $p_{s,av.1}$, which is represented by the logarithmic mean value of the applied consolidation pressure p_2 and the initial solid compressive pressure p_1 of homogeneous semi-solid materials, as defined by

$$p_{s,av.1} = \frac{p_2 - p_1}{\ln(p_2/p_1)} \quad (6)$$

In Figure 6, C_c obtained from the experimental data at various values of consolidation pressure p_2 and salt concentration C_0 is plotted against $p_{s,av.1}$. The plots scattered because they are strongly affected by the salt concentration C_0 . The results imply that the effect of the osmotic pressure associated with the salt plays an important role in describing the dynamic behaviors of consolidation of packed hydrogels.

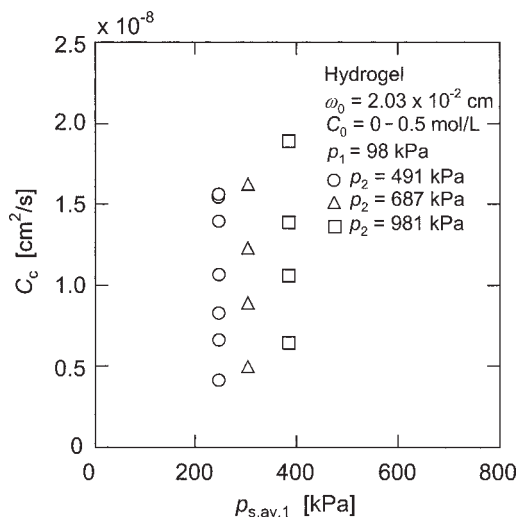


Figure 6. Influence of applied consolidation pressure p_2 on modified consolidation coefficient C_c .

To analyze the transient response of the consolidation of packed hydrogels to changes in the salt concentration, it becomes first necessary to evaluate the effect of the addition of salt on the equilibrium state of the packed hydrogels under the solid compressive pressure. Figure 7 shows a logarithmic plot of the final equilibrium average solidosity (volume fraction of solids) $(1 - \epsilon_{av,\infty})$ in the compressed cake of hydrogels swelled by pure water alone vs. the applied mechanical consolidation pressure p_2 , where $\epsilon_{av,\infty}$ is related to the final equilibrium average void ratio $e_{av,\infty}$ by $\epsilon_{av,\infty} = e_{av,\infty}/(1 + e_{av,\infty})$. As the consolidation pressure increases, hydrogels forming the cake are compressed, resulting in the increase in the solidosity. The plots show a linear relationship. Thus, over the range of pressure examined in this study, the relation takes the empirical form

$$1 - \epsilon_{av,\infty} = E p_2^\beta \quad (7)$$

where $\epsilon_{av,\infty}$ is the final equilibrium average porosity of the compressed cake and E and β are the empirical fitting parameters. As p_2 approaches zero, Eq. 7 must be abandoned because it yields zero for $\epsilon_{av,\infty}$. Experimentally, $\epsilon_{av,\infty}$ approaches a limiting value that is defined as ϵ_i . Below pressure p_i , the porosity is assumed constant.¹⁷ Term β is an indication of the compressibility of the compressed cake and is determined from the slope of the line in Figure 7. The larger the value of β , the higher the compressibility. The value of β for the packed hydrogels examined in this study was determined to be about 0.95. Given that it is reported that the value of β for kaolin with moderate compressibility is 0.054,^{17,18} it is considered that the packed hydrogels are highly compactible materials, with hydraulic permeability decreasing dramatically with increasing applied pressure. In general, the side friction^{19,20} between the compressed cake and the wall of the C-P cell often affects the uniformity of the cake packing. In this study, the ratio (L/D) of the cake thickness in consolidation and expansion processes to cell diameter was maintained at low values ranging from 0.028 to 0.139 to justify the

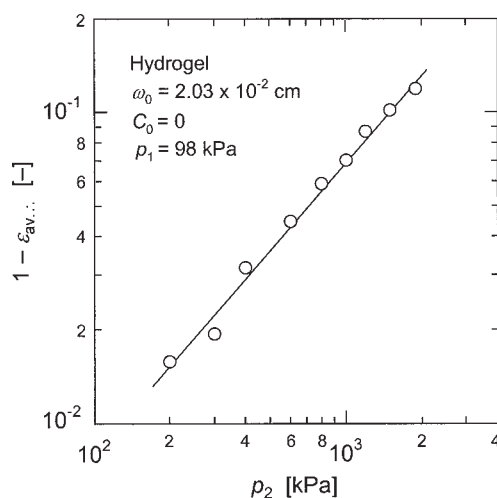


Figure 7. Relation between final equilibrium average solidosity $(1 - \epsilon_{av,\infty})$ of compressed cake of hydrogels swelled by pure water and applied consolidation pressure p_2 .

coarse assumption that the side friction is negligible. It should thus be noted that the solidosity is approximated to be constant throughout the compressed cake under a given condition of the consolidation pressure at the equilibrium state of consolidation.

Figure 8 shows the changes in the final equilibrium average solidosity ($1 - \varepsilon_{av,\infty}$) of the compressed cake of hydrogels with the salt concentration C_0 . It is clear that the solidosity remarkably increases in response to an increase in the salt concentration C_0 . When the salts are contained in the granular bed of hydrogels, the final equilibrium average solidosity increases further under the influence of the osmotic pressure of the salt solution. Moreover, because the sodium ions dissociated from the functional groups in the gel ($-\text{COONa}$) are easily exchanged with the other cations in the solution, this additional influence must be considered.²¹

To quantitatively deal with these complex phenomena caused by the addition of the salt, the idea of effective osmotic pressure of the solution has been proposed in this work. It is supposed that the effective osmotic pressure Π_{ef} caused by the salt equals the additional mechanical pressure ($p - p_2$) that gives the same equilibrium average solidosity ($1 - \varepsilon_{av,\infty,1}$) as that attained by the salt, as schematically shown in Figure 9. Consequently, the effective osmotic pressure Π_{ef} can be evaluated by comparing the data of Figure 8 with those of Figure 7. The effective osmotic pressure Π_{ef} thus obtained is shown in Figure 10 as a function of the salt concentration C_0 . It is found that the effective osmotic pressure Π_{ef} undergoes a rapid increase initially and then increases more slowly with C_0 . The dashed line represents the real osmotic pressure of the added salt solution,²² and the pressure appears to increase almost linearly with the increase in C_0 . The effective osmotic pressure Π_{ef} lies below the real osmotic pressure represented by the dashed line and the difference between both pressures becomes considerable as the salt concentration C_0 increases. What is interesting to note here is that almost the same effective osmotic pressure Π_{ef} is obtained for the same salt concentration C_0 , even though the consolidation pressure p_2 is different, as shown in the figure.

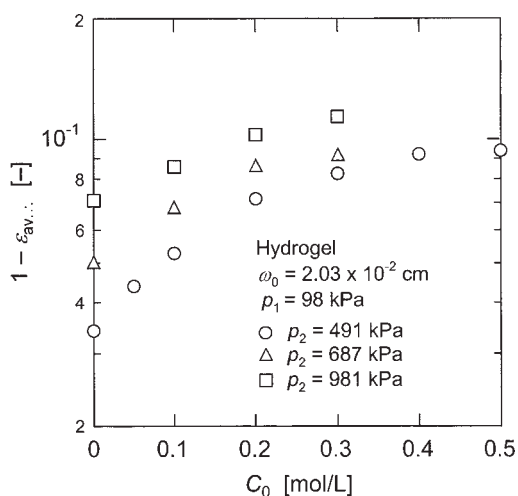


Figure 8. Influence of salt concentration C_0 on final equilibrium average solidosity ($1 - \varepsilon_{av,\infty}$).

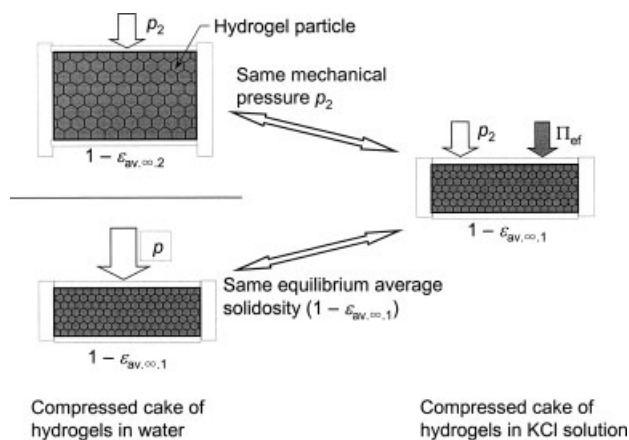


Figure 9. Method for determining effective osmotic pressure of solution arising from addition of salt.

The transient behaviors of consolidation can also be described using the effective osmotic pressure Π_{ef} determined from the comparison of the average solidosity of the compressed cake at the equilibrium state of consolidation. Figure 11 shows the modified consolidation coefficient C_c as a function of the effective average solid compressive pressure $p_{s,av,2}$ for various salt concentrations, where $p_{s,av,2}$ is the logarithmic mean value of $(p_2 + \Pi_{\text{ef}})$ and $(p_1 + \Pi_{\text{ef}})$, as defined by

$$p_{s,av,2} = \frac{p_2 - p_1}{\ln[(p_2 + \Pi_{\text{ef}})/(p_1 + \Pi_{\text{ef}})]} \quad (8)$$

This equation indicates that the effective osmotic pressure Π_{ef} of the solution enters into the calculation of the effective average solid compressive pressure $p_{s,av,2}$. Interestingly, the data collapse to nearly a single line through the origin, irre-

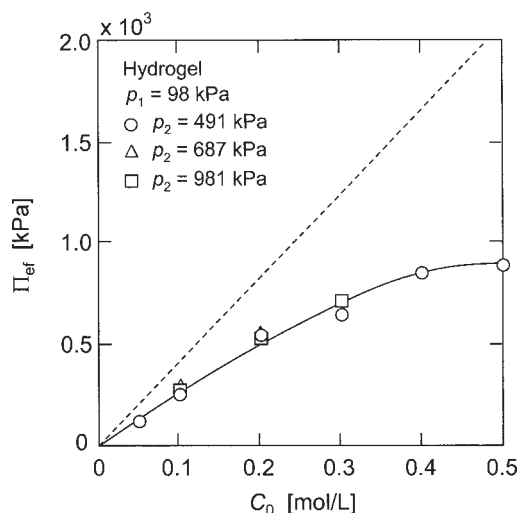


Figure 10. Relation between effective osmotic pressure Π_{ef} and salt concentration C_0 .

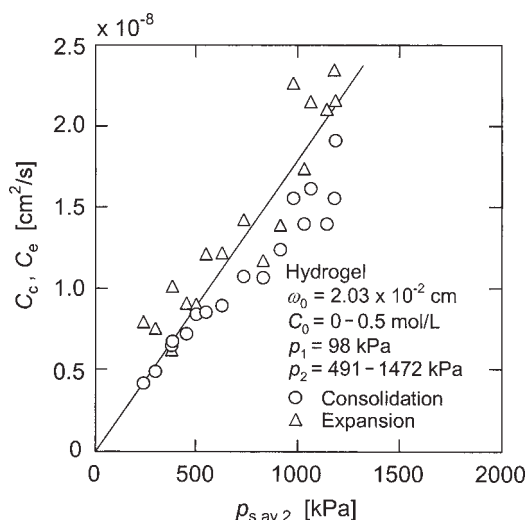


Figure 11. Dependency of both modified consolidation coefficient C_c and modified expansion coefficient C_e on effective average solid compressive pressure $p_{s,av,2}$.

spective of the salt concentration, when plotted in this manner. It is demonstrated that the transient behavior of consolidation can be well described analytically on the basis of the data of the equilibrium state of consolidation by introducing the idea of the effective osmotic pressure of the solution.

Figure 12 compares the experimental data with the calculations of the variations with time of the average void ratio e_{av} of the compressed cake during the course of a consolidation period at various values of the salt concentration C_0 and the consolidation pressure p_2 , demonstrating an excellent correlation. The time variations of e_{av} were evaluated as subsequently discussed. For the condition of a given salt concen-

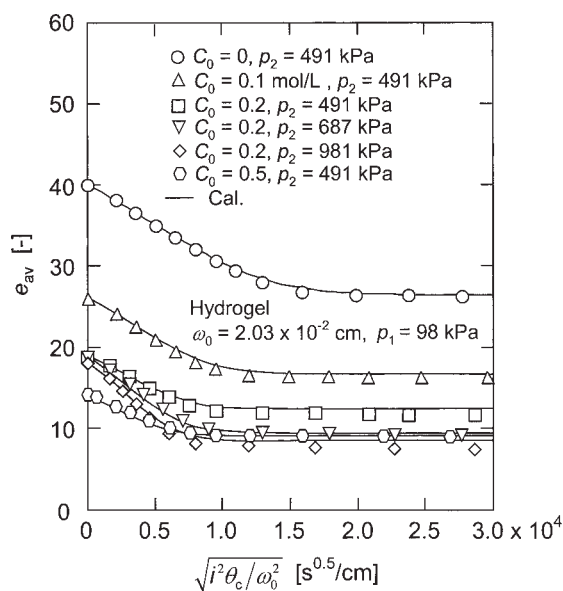


Figure 12. Evaluation of variations of average void ratio e_{av} of cake with time during consolidation.

tration, the effective osmotic pressure Π_{ef} can be obtained by using the relation shown in Figure 10. Because the effective average solid compressive pressure $p_{s,av,2}$ can be calculated from Eq. 8, the modified consolidation coefficient C_c can be determined on the basis of the relation shown in Figure 11. Consequently, the time variation of the average consolidation ratio U_c can be evaluated from Eq. 1. The time variation of the average void ratio e_{av} of the compressed cake can also be calculated from Eq. 5 using the average consolidation ratio U_c thus obtained as the input. Using the value of $e_{av,\infty}$ determined based on the compression data shown in Figure 7 in consideration of the effective osmotic pressure Π_{ef} , the value of the equilibrium thickness L_∞ of the compressed cake that appears in Eq. 5 may be obtained from

$$L_\infty = \frac{1 - \varepsilon_{av,1}}{1 - \varepsilon_{av,\infty}} L_1 \quad (9)$$

where $\varepsilon_{av,1}$ represents the average porosity of the compressed cake at the beginning of consolidation.

On the basis of the idea of the effective osmotic pressure of the solution, the consolidation time $\theta_{c,90}$ required for attaining 90% of the average consolidation ratio U_c can be calculated against various conditions of the consolidation pressure p_2 and the salt concentration C_0 , as illustrated in Figure 13. The consolidation time $\theta_{c,90}$ is largely influenced by the consolidation pressure p_2 when the salt concentration C_0 is low, but the time $\theta_{c,90}$ is relatively scarcely affected by the pressure p_2 at the high salt concentration.

Expansion behaviors of packed hydrogels

Figure 14 shows the typical results obtained in expansion of the packed bed of the swelled superabsorbent hydrogels. The homogeneous semisolid material that was consolidated at a constant pressure of 491 kPa was expanded at a pressure of 98 kPa after a partial release of the load under various conditions of salt concentration. The average expansion ratio

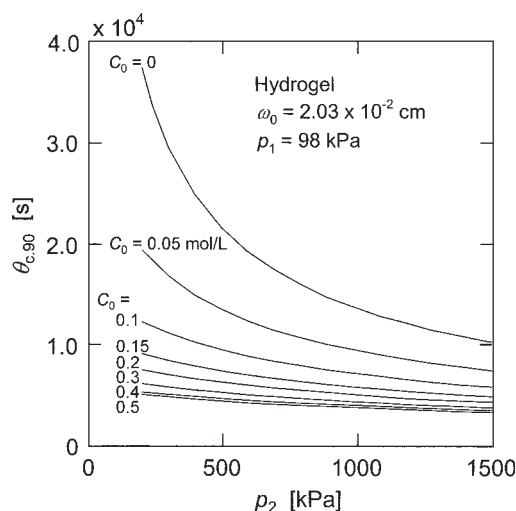


Figure 13. Influence of consolidation pressure p_2 and salt concentration C_0 on consolidation time $\theta_{c,90}$ for attaining 90% of average consolidation ratio U_c .

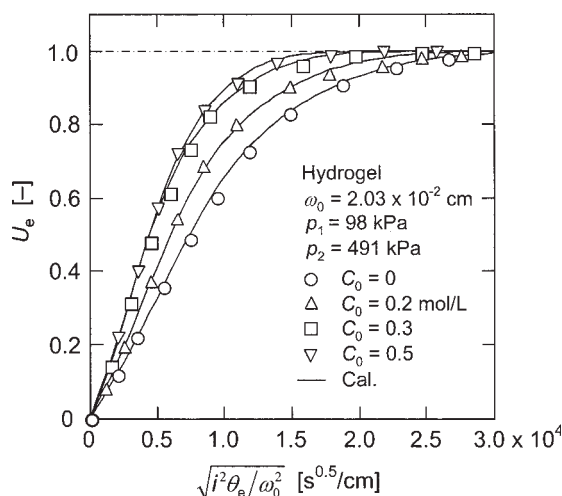


Figure 14. Evaluation of average expansion ratio U_e based on Terzaghi-Voigt combined model.

U_e was plotted against the square root of $i^2 \theta_e / \omega_0^2$ for the different salt concentrations, where θ_e is the expansion time. The average expansion ratio U_e is defined as $U_e = (L_1 - L) / (L_1 - L_\infty)$ in the expansion process as well as in the case of consolidation, where L_1 , L , and L_∞ are, respectively, the thickness of the compressed cake at the expansion time $\theta_e = 0$, $\theta_e = \theta_e$, and $\theta_e = \infty$. The average expansion ratio U_e was equal to zero at the start of expansion and gradually approached unity with the progress of expansion. The figure shows that expansion proceeds more quickly as the salt concentration increases and that, at a concentration > 0.3 mol/L, the expansion rate is only negligibly influenced by the salt concentration, in the same way as the case of consolidation. It was also noticeable, however, from the comparison with Figure 2 that expansion proceeds more slowly than consolidation, as previously reported²³ for the absence of the salt. Because the calculations based on the modified Terzaghi model used in the analysis of the consolidation process led to erroneous results in the estimation of the experimental data, not only the primary expansion—which occurs simultaneously with a decrease in local solid compressive pressure p_s —but also the creep effect of secondary expansion must be accounted for. Based on the Terzaghi-Voigt combined model,¹⁴ which may be represented by a spring in series with a unit that consists of a spring in parallel with a dash-pot, an explicit equation for the average expansion ratio U_e as a function of expansion time θ_e for constant-pressure expansion of homogeneous semisolid materials may be presented in the form²³

$$U_e = (1 - B) \left\{ 1 - \sum_{N=1}^{\infty} \frac{8}{(2N-1)^2 \pi^2} \exp \left[-\frac{(2N-1)^2 \pi^2 i^2 C_e \theta_e}{4 \omega_0^2} \right] \right\} + B[1 - \exp(-\eta \theta_e)] \quad (10)$$

where C_e is the modified expansion coefficient, B is the creep constant representing the ratio of the secondary expansion to the total expansion, and η is the creep constant

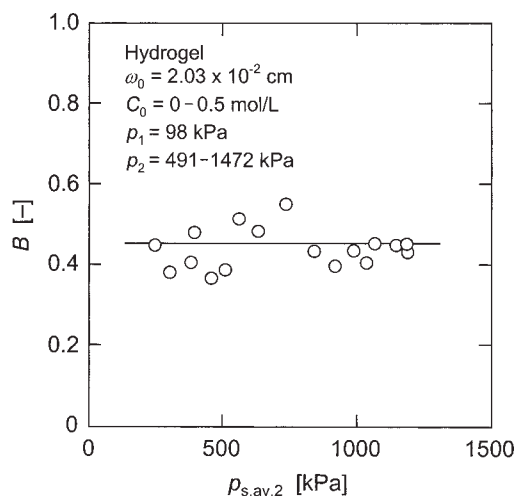


Figure 15. Relation between creep constant B and effective average solid compressive pressure $p_{s.av.2}$.

defined by the ratio of the elastic coefficient of the spring of the Voigt model to the viscosity of the dash pot of the Voigt model. The overall fits to the data are quite excellent throughout the entire course of expansion. This implies that consideration of the creep effect, known as the secondary expansion effect, adequately estimates the observed results of expansion of packed hydrogels. This creep effect probably arises from the slow rearrangement of the tightly packed hydrogel particles constrained within the compressed cake in response to the decrease in the applied pressure.

In Figures 15 and 16, the creep constants B and η in Eq. 10 obtained by the fitting method proposed by Shirato et al.¹⁴ are respectively plotted against the effective average solid compressive pressure $p_{s.av.2}$ defined by Eq. 8 for various values of the initial pressure p_2 and the salt concentration C_0 . Although there is some scatter in the ratio B of the secondary

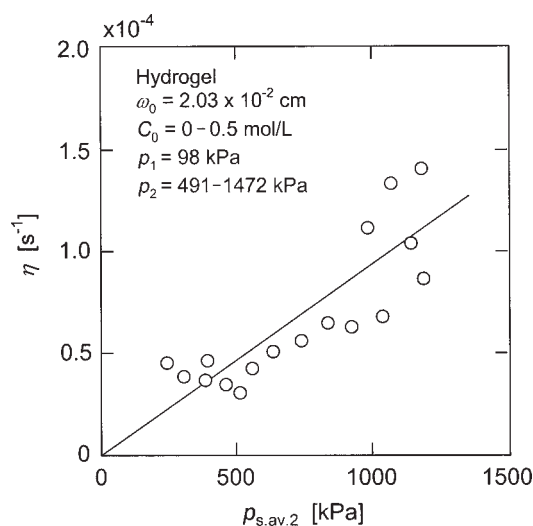


Figure 16. Relation between creep constant η and effective average solid compressive pressure $p_{s.av.2}$.

expansion to the total expansion, the ratio B ranges from 0.37 to 0.54. Thus, the effect of the secondary expansion is significant. In addition, the creep constant η increases roughly with increasing $p_{s,av,2}$.

Use of the following semitheoretical equation instead of Eq. 10 permits a simplification:

$$U_e = \sqrt{\frac{4 i^2 C_e \theta_e}{\pi \omega_0^2}} \left/ \left[1 + \left(\frac{4 i^2 C_e \theta_e}{\pi \omega_0^2} \right)^{\nu} \right]^{1/(2\nu)} \right. \quad (11)$$

In Figure 17, the experimental data indicated in Figure 14 are compared with calculations based on Eq. 11. The model calculations are shown as the solid curves, with the best fit values of $\nu = 2.0$ for the conditions of all the salt concentrations. It was previously reported that the value of ν provides a good measure of the creep effect.¹⁵ The overall fits to the data are quite excellent, suggesting that consideration of the creep effect provides a reasonable description of the expansion of packed hydrogels.

Figure 18 shows the variations of the average void ratio e_{av} of the cake with expansion time θ_e during the expansion period at various salt concentrations. Initially, the values of e_{av} increase rapidly with time and approach the equilibrium values asymptotically. As the salt concentration increases, e_{av} becomes substantially smaller and the variation of e_{av} is not noticeable. The solid curves are the calculations obtained by a manner similar to the analysis of consolidation used in Figure 4.

Also, in the analysis of the expansion of the granular bed of hydrogel particles, it is highly beneficial to introduce the idea of the effective osmotic pressure of the solution. In Figure 11, the modified expansion coefficient C_e is also plotted against the average solid compressive pressure $p_{s,av,2}$, defined by Eq. 8 for various values of the salt concentration C_0 and the pressure p_2 . The plots yield a straight line through the origin, irrespective of the salt concentration C_0 and pressure p_2 . Of particular importance is that the plots for C_e indicating the primary expansion rate are in relatively good agreement with those for C_c indicating the primary consolidation rate.

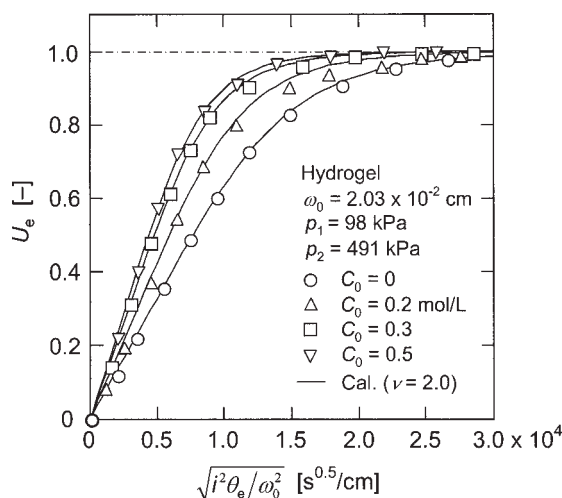


Figure 17. Evaluation of average expansion ratio U_e based on simplified computation method.

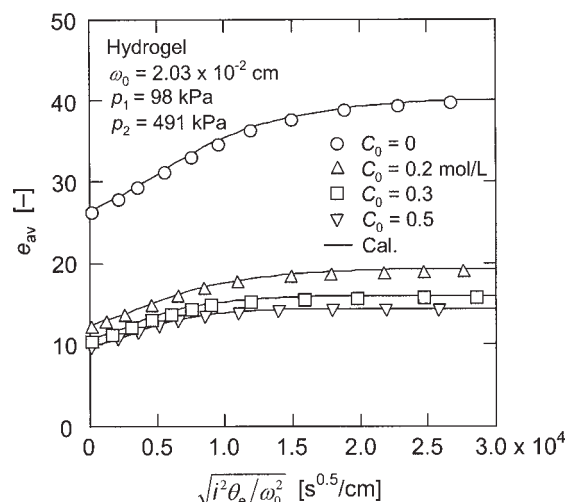


Figure 18. Variations of average void ratio e_{av} of cake with time during expansion.

However, expansion proceeds more slowly than consolidation, reflecting the significant creep effect in expansion.

Conclusions

The global behaviors of consolidation and expansion of the granular bed of superabsorbent hydrogel particles with varying mechanical load and solution environments were examined by using either the modified Terzaghi model, the Terzaghi–Voigt model, or the simplified computation method. Introducing the idea of the effective osmotic pressure of the solution can provide a very good description of the complex effects of the addition of salt on both the consolidation and expansion behaviors. As the salt concentration increases, the hydrogel particles dramatically shrink in volume, leading to the small average void ratio of the compressed cake. In the consolidation process, the creep effect is negligible, whereas in the expansion process it is pronounced. Moreover, it is found that expansion proceeds more slowly than consolidation. The results obtained in this work provide important new insights into the mechanisms involved in the deformation of packed hydrogels under the influences of the mechanical pressure and the ionic environment of the solution.

Acknowledgments

This work was partially supported by a Grant-in-Aid for Scientific Research from The Ministry of Education, Culture, Sports, Science and Technology, Japan. The authors gratefully acknowledge the financial support leading to the publication of this article. The authors also thank H. Y. Lee for assistance in carrying out the experiments.

Notation

- B = creep constant representing ratio of secondary expansion to total expansion
- C_0 = salt concentration, mol/L
- C_c = modified consolidation coefficient, m^2/s
- C_e = modified expansion coefficient, m^2/s
- D = inner diameter of C-P cell cylinder, m

E = empirical parameter defined by Eq. 7, $\text{Pa}^{-\beta}$
 e = local void ratio of cake
 e_{av} = average void ratio of cake
 $e_{\text{av},\infty}$ = final equilibrium average void ratio of cake at $\theta_c = \infty$
 i = number of drainage surfaces
 L = thickness of cake, m
 L_1 = thickness of cake at $\theta_c = 0$ or $\theta_e = 0$, m
 L_{∞} = final equilibrium thickness of cake at $\theta_c = \infty$ or $\theta_e = \infty$, m
 p = applied pressure, Pa
 p_1 = preconsolidation pressure, or pressure after partial release of load, Pa
 p_2 = consolidation pressure, or pressure before partial release of load, Pa
 p_i = low consolidation pressure below which equilibrium porosity is constant, Pa
 p_s = local solid compressive pressure, Pa
 $p_{\text{s.av.1}}$ = average solid compressive pressure defined by Eq. 6, Pa
 $p_{\text{s.av.2}}$ = effective average solid compressive pressure defined by Eq. 8, Pa
 U_c = average consolidation ratio
 U_e = average expansion ratio

Greek letters

α = local specific resistance of material, m/kg
 β = empirical parameter defined by Eq. 7
 $\varepsilon_{\text{av.1}}$ = average porosity of cake at $\theta_c = 0$
 $\varepsilon_{\text{av},\infty}$ = final equilibrium average porosity of cake at $\theta_c = \infty$
 $\varepsilon_{\text{av},\infty.1}$ = final equilibrium average porosity of cake at $\theta_c = \infty$ under pressure p shown in Figure 9
 $\varepsilon_{\text{av},\infty.2}$ = final equilibrium average porosity of cake at $\theta_c = \infty$ under pressure p_2 shown in Figure 9
 ε_i = value of equilibrium porosity when consolidation pressure is smaller than p_i
 η = creep constant defined by ratio of elastic coefficient of spring of Voigt model to viscosity of dash pot of Voigt model, s^{-1}
 θ_c = consolidation time, s
 θ_e = expansion time, s
 μ = viscosity of liquid, Pa·s
 ν = consolidation behavior index in Eq. 4 or expansion behavior index in Eq. 11
 ρ_s = true density of solids, kg/m^3
 Π_{ef} = effective osmotic pressure of solution, Pa
 ω_0 = total solid volume per unit cross-sectional area, m^3/m^2

Literature Cited

- Nakano Y, Seida Y, Uchida M, Yamamoto S. Behavior of ions within hydrogel and its swelling properties. *J Chem Eng Jpn.* 1990;23:574–579.
- Shirato M, Murase T, Kato H, Fukaya S. Studies on expression of slurries under constant pressure. *Kagaku Kogaku.* 1967;31:1125–1131.
- Yukawa H, Suda H, Hoshino T. Rheological characteristics of gelatin gel for compressive stress. *Kagaku Kogaku Ronbunshu.* 1985;11:855–861.
- Nakakura H, Sambuichi M, Ishitoku H, Osasa K. Filtration mechanism of gel particle slurry. *J Chem Eng Jpn.* 2001;34:862–868.
- Schwartzberg HG. Expression of fluid from biological solids. *Sep Purif Methods.* 1997;26:1–213.
- Sambuichi M, Nakakura H, Nishigaki F, Osasa K. Dewatering of gels by constant pressure expression. *J Chem Eng Jpn.* 1994;27:616–620.
- Lanoisellé JL, Vorobyov EI, Bouvier JM, Piar G. Modeling of solid/liquid expression for cellular materials. *AIChE J.* 1996;42:2057–2068.
- Chang IL, Lee DJ. Ternary expression stage in biological sludge dewatering. *Water Res.* 1998;32:905–914.
- Badiger MV, Lele AK, Kulkarni MG, Mashelkar RA. Swelling and phase transitions in deforming polymeric gels. *Ind Eng Chem Res.* 1994;33:2426–2433.
- Tanaka T, Hocker LO, GB Benedek. Spectrum of light scattered from a viscoelastic gel. *J Chem Phys.* 1973;59:5151–5159.
- Iwata M, Koda S, Nomura H. Theory of compression and expansion of hydrogels. *J Chem Eng Jpn.* 1999;32:684–688.
- Lu WM, Tung KL, Hung SM, Shiau JS, Hwang KJ. Compression of deformable gel particles. *Powder Technol.* 2001;116:1–12.
- Grace HP. Resistance and compressibility of filter cakes, Part I. *Chem Eng Prog.* 1953;49:303–318.
- Shirato M, Murase T, Tokunaga A, Yamada O. Calculations of consolidation period in expression operations. *J Chem Eng Jpn.* 1974;7:229–231.
- Shirato M, Murase T, Atsumi K, Aragaki T, Noguchi T. Industrial expression equation for semi-solid materials of solid-liquid mixture under constant pressure. *J Chem Eng Jpn.* 1979;12:51–55.
- Sivaram B, Swamee PK. A computational method for consolidation-coefficient. *J Jpn Soc Soil Mech.* 1977;17:48–52.
- Tiller FM, Cooper H. The role of porosity in filtration: Part V. Porosity variation in filter cakes. *AIChE J.* 1962;8:445–449.
- Shirato M, Okamura S. Behaviors of various kaolin slurries in constant pressure filtration (about Hongkong kaolins, “pink” and “dark yellow,” and Shinmei kaolin). *Kagaku Kogaku.* 1959;23:11–17.
- Shirato M, Aragaki T, Mori R, Sawamoto K. Predictions of constant pressure and constant rate filtrations based upon an approximate correction for side wall friction in compression permeability cell data. *J Chem Eng Jpn.* 1968;1:86–90.
- Tiller FM, Haynes S, Lu WM. The role of porosity in filtration: VII. Effect of side-wall friction in compression-permeability cells. *AIChE J.* 1972;18:13–20.
- Sakohara S, Muramoto F, Asaeda M. Swelling and shrinking processes of sodium polyacrylate-type super-absorbent gel in electrolyte solutions. *J Chem Eng Jpn.* 1990;23:119–124.
- Money NP. Osmotic pressure of aqueous polyethylene glycols. Relationship between molecular weight and vapor pressure deficit. *Plant Physiol.* 1989;91:766–769.
- Murase T, Iwata M, Wakita M, Adachi T, Hayashi N, Shirato M. Expansion of consolidated material after release of load. *J Chem Eng Jpn.* 1989;22:195–199.

Manuscript received Apr. 26, 2006, and revision received Aug. 31, 2006.